New developments in the study of binary fluids under shear flow

D. Beysens, M. Gbadamassi,* and B. Moncef-Bouanz†
Service de Physique du Solide et de Résonance Magnétique, Division de la Physique, Commissariat à l'Energie Atomique, Centre d'Etudes Nucléaires de Saclay, F-91191 Gif-sur-Yvette Cedex, France
(Received 6 December 1982)

Three binary fluids, aniline-cyclohexane, nitrobenzene-*n*-hexane, and isobutyric acid—water, have been studied by light scattering and turbidity techniques near their critical points, both at the thermodynamic equilibrium and under a shear flow, as a function of the variables temperature T, relative concentration M, shear rate S, and wave vector $\vec{q}$. The following results have been obtained: (i) *Out of equilibrium.* The region where a shear affects the critical behavior has been determined in the plane (M,T); the crossover temperature varies as M^2, and the coexistence curve exhibits the classical exponent ($\beta=\frac{1}{2}$). A small temperature change due to the shear was detected; its value is about four times lower than that calculated by the Onuki-Kawasaki theory. The susceptibility versus T, M, S, and $\vec{q}$ is well represented by the Onuki-Kawasaki formulation, in particular the exponent γ shows the classical value ($\gamma=1$). (ii) *At equilibrium.* The susceptibility and the correlation length have been measured on the critical isochore above T_c, on the coexistence curve, and on the critical isotherm. The universal amplitude ratios ξ_0^+/ξ_0^-, C^+/C^-, R_χ^+, and Q_2 have been obtained. The typical time taken by the system to return to equilibrium after having been perturbed by shear has been analyzed in terms of mass diffusion.

I. INTRODUCTION

Binary fluids may exhibit a liquid-liquid critical point at the critical concentration $c=c_c$, and near this second-order phase transition their thermodynamic and correlation properties show universal behaviors. With respect to critical phenomena, binary fluids belong to the same universality class as pure fluids or the three-dimensional (3D) Ising model, a class characterized by the dimensionality of the physical space ($d=3$) and by a scalar order parameter ($N=1$); here the order parameter is the relative concentration $M=c-c_c$. The critical behavior of such systems seems now to be well understood at thermodynamic equilibrium.[1]

It is only recently that critical fluids out of equilibrium have begun to be studied, especially binary fluids under shear flow. Theory[2] and experiment[3] have been worked out at the same time. The main result lies in the change of behavior near the critical point: Mean-field theory becomes relevant, whereas it should have been valid for the same systems at equilibrium only in a space with dimensionality d higher than 4.

Although the agreement between theory and experiment might have been regarded as satisfactory,[2(c),3(a),3(b)] some problems[3(c)] still remain, mainly owing to the use in the first experiments of a continuously varying shear. Moreover, the order parameter behavior was not investigated. The aim of the present paper is therefore as follows.

(i) To check the universality of the phenomena by considering various physical systems. Besides the aniline-cyclohexane (*A-C*) mixture already studied, we have also considered the isobutyric acid—water (*I-W*) and nitrobenzene-*n*-hexane (*N-H*) systems.

(ii) To check the order parameter influence. In particular, does the transition under shear remain second order? Is there any critical concentration shift? Obtaining the critical exponent β is of great interest since the classical value $\frac{1}{2}$ is expected. We will see below that such a study also allows us to obtain some equilibrium properties which have not yet been obtained in binary fluids, such as the correlation length and the susceptibility along the critical isotherm.

(iii) To directly determine the critical temperature shift through the susceptibility divergence. This was made possible only because a new cell producing a nearly constant shear rate was built. The results so obtained somewhat modify the interpretation of already published works.

(iv) To investigate as a function of time the reestablishment of equilibrium properties when shear is

suddenly stopped.

This paper is organized as follows: First, the theoretical background, with emphasis on the simplifications we had to make to interpret the data; second, the experimental part, where only the new features are reported; third, the results and their discussion. A special section will be devoted to the properties at equilibrium, determined as a by-product of this study. Finally, we will include in the conclusion a rapid survey of the most significant results.

II. THEORETICAL BACKGROUND

Most of the out of equilibrium theoretical work is owing to Onuki and Kawasaki (OK).[2] However, before entering into the details of the OK approach, and in order to give a comprehensive view of the phenomenon, we present a phenomenological description.

A. Phenomenology—Generality

Let us imagine, for sake of simplicity, that the order-parameter fluctuations at equilibrium look like spherical droplets. These droplets represent the correlation volumes, whose size is characterized by the correlation length ξ. Let us assume that in a given droplet an excess of concentration is found. Let us now apply shear. Only the volume elements of the droplet which are in the shear direction will be shifted, so that an excess of concentration will remain only in the plane perpendicular to the shear, in the direction of flow. The first effect of shear is therefore to destroy the correlations in the shear direction, making the fluctuations anisotropic.

What is the frontier between the regime of "weak shear," where droplets are only slightly anisotropic, and "strong shear," where correlations are strongly reduced? This crossover will occur when the lifetime (τ) of fluctuations is large enough to "feel" the shear. With S the shear rate, this will occur for a shift ($\xi S\tau$) in the shear direction greater than the typical length ξ of the droplets, i.e., "strong shear" means

$$S\tau > 1 \ . \tag{1}$$

The lifetime τ of a cluster of radius ξ moving in a medium of viscosity η is classically[4]

$$\tau = \frac{16\eta}{k_B T}\xi^3 \tag{2}$$

with k_B the Boltzmann constant and T the absolute temperature. ξ diverges near the critical temperature T_c as

$$\xi = \xi_0 t^{-\nu} \ , \tag{3}$$

where $t=(T-T_c)/T_c$, $\nu=0.630$ is the universal exponent,[1] and ξ_0 is an amplitude. The condition $S\tau>1$ can therefore be written as a temperature condition:

$$T < T_s \ ,$$

where T_s is the crossover temperature, whose value, according to (2) and (3), is

$$T_s = T_c \left[1 + \left[\frac{16\eta\xi_0^3}{k_B T_c} \right]^{1/3\nu} S^{1/3\nu} \right] . \tag{4}$$

In the strong shear region the concentration fluctuations are anisotropic. This leads to a corresponding anisotropy in the order parameter susceptibility. The divergence of this susceptibility determines the critical temperature under shear T_c^*. Since, at least at first order, fluctuations are only weakly affected in the direction of flow, we expect a weak change, $T_c^* \simeq T_c$.

However, at the same distance from the critical point, the sheared fluctuations of the order parameter are greatly reduced when compared to their equilibrium level. The Ginzburg criterion[5] can then be fulfilled, and mean-field behavior becomes relevant.

A more rigorous theory by OK[2] leads to the same conclusions. However, quantitative predictions—including the influence of a non-zeroth order parameter—have been made, and these will now be considered.

B. Coexistence curve: Strong shear region in the plane (M,T)

In the following we will consider the same properties at equilibrium or under shear. We will then use the same letters and denote the out-of-equilibrium properties by an asterisk.

In the region of strong shear, the equation of state is classical according to OK. The coexistence curve therefore exhibits a mean-field behavior with exponent $\beta^* = \frac{1}{2}$:

$$M^* = B_0^* (-t^*)^{\beta^*} \ . \tag{5}$$

Here B_0^* is the amplitude, and $M^* = c - c_c^*$ with c_c^* the critical composition under shear. One expects $c_c^* = c_c$; $t^* = (T_\varphi^* - T_c^*)/T_c^*$, where T_φ^* is the phase transition temperature under shear.

At equilibrium,

$$M = B_0 (-t)^{\beta} \tag{6}$$

with $\beta=0.325$, a universal exponent.[1]

The critical temperature T_c^* is expected to be a

function of the crossover temperature T_s, defined above in (4):

$$T_c^* - T_c = -v(T_s - T_c) . \tag{7}$$

v is a numerical constant; according to OK,

$$v \simeq 8.32 \times 10^{-2} .$$

The crossover temperature $T_s(M)$ can be determined through the condition $S\tau = 1$. τ is related to ξ by (2). Using the approximate expression cited by OK in Ref. 2(b),

$$\xi^{-2} = t\xi_0^{-2}(\xi\xi_0^{-1})^{-1/3} + \tfrac{1}{2}u^* M^2 \xi_0^{-1}\xi^{-1} , \tag{8}$$

where $u^* = 4\pi^2/3$, the condition of strong shear becomes

$$M = \left[\frac{2}{u^*}\right]^{1/2}\left[\frac{16\eta\xi_0^3 S}{k_B T}\right]^{-1/9}\left[\frac{T_s - T_s(M)}{T_c}\right]^{1/2} . \tag{9}$$

Here the classical value $\frac{1}{2}$ is not related to the strong shear regime itself, but to the M variation of the approximation (8).

Finally, the strong shear region in the plane (M,T) will be delimited by $T_s(M)$ and the coexistence curve $T_\varphi(M)$, as shown in Fig. (1).

C. Correlation length and susceptibility

The concentration fluctuations are strongly coupled to the refractive index and then give rise to an intense light scattering phenomenon. The intensity of light scattered at a given transfer wave vector q is merely the order parameter susceptibility at the same wave vector,[1,6]

$$\chi_q(t) = \chi(t)G(q\xi) . \tag{10}$$

$\chi(t)$ is the $q=0$ susceptibility, and $G(q\xi)$ is the Fourier transform of the normalized correlation function, well described by the function, where $X = q\xi$ (Ref. 7)

$$G(X) = \sum_{i=1}^{3} c_i(1 + a_i^2 X^2)^{-b_i} . \tag{11}$$

Here $a_1 = 1.040\,056$, $a_2 = 1.058\,947$, $a_3 = 1.053\,932$, $b_1 = 0.984\,25$, $b_2 = 1.554\,213$, $b_3 = 1.627\,419$, and $c_1 = c_2 = -c_3 = 1$.

From (10) both χ and ξ can be deduced.

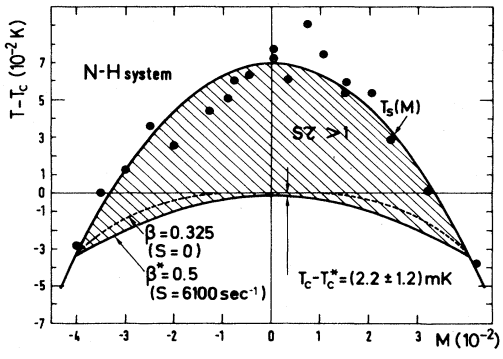

FIG. 1. Region of strong shear ($S\tau > 1$) in the plane (M,T) for the N-H system and for a shear $S = 6100\ \text{sec}^{-1}$. The upper line corresponds to the crossover temperature $T_s(M)$ which varies as M^2. The lower line is the coexistence curve under shear with the classical exponent $\beta^* = \frac{1}{2}$. The hatched line is the coexistence curve at equilibrium with exponent $\beta = 0.325$.

1. At equilibrium

The conjugate field of the order parameter is here the chemical potential difference $\mu = \mu_1 - \mu_2$ of the components. Along the critical isochore $t > 0$, $M = \mu = 0$, the following dependences pertain as[1]

$$\text{susceptibility } \chi = \left[\frac{\partial c}{\partial \mu}\right]_{p,T} = C^+ t^{-\gamma}/k_B T_c , \tag{12}$$

$$\text{correlation length } \xi = \xi_0^+ t^{-\nu} . \tag{13}$$

Along the critical isotherm ($t = 0$), whose equation is

$$\mu = DM^\delta , \tag{14}$$

we have

$$k_B T\chi = C_c \mu^{-\gamma/\beta\delta} \equiv \frac{1}{\delta D^{1/\delta}}\mu^{-\gamma/\beta\delta} , \tag{15}$$

using the definition $C_c = 1/\delta D^{1/\delta}$.

Also

$$\xi = \xi_0^c \mu^{-\nu/\beta\delta} . \tag{16}$$

Along the coexistence curve ($\mu = 0$, $t < 0$), whose equation is (6), we have

$$k_B T\chi = C^-(-t)^{-\gamma} \tag{17}$$

and

$$\xi = \xi_0^-(-t)^{-\nu} . \tag{18}$$

All these formulas hold asymptotically close to the critical point. Further away, multiplicative corrective factors of the form

$$(1 + a_1 t^\Delta + \cdots) \tag{19}$$

must be introduced.[1] They are negligible in this study, which was carried out very close to T_c.

The values admitted for the exponents[1] are $\gamma=1.240$, $\nu=0.630$, $\beta=0.325$, $\delta=4.815$, and $\Delta=0.50$.

One notes that in the usual Ornstein-Zernike approximation of $G(q\xi)$, where $\gamma\simeq 2\nu$, the q susceptibility on the critical isochore exhibits the simple form,

$$\chi_q^{-1}=At^{\gamma}+q^2 \tag{20}$$

with $A=\xi_0^{-2}$ and where the multiplicative constant factor C/ξ_0^2 has been omitted. The critical temperature can be therefore experimentally determined by extrapolating at zero the values of χ_q^{-1} versus T, provided that the experiments were performed at very small q.

2. *Out of equilibrium*

Let us consider a flow in X direction, with a linear velocity gradient in the Y direction $[V(Y)]$ (Fig. 2). The shear rate is $S=\partial V/\partial Y\simeq$const. A laser beam is directed along Z, perpendicularly to the flow and the shear. Under these conditions, the susceptibility to be measured can be described to within (20—30)% as the sum of 4 contributions (the simplification $\gamma\simeq 2\nu$ has been made):

$$(\chi_q^*)^{-1}=A^*t^{*\gamma^*}+E^*M^{*\delta^*-1}+B^*q_X^{0.4}+q^2 \ . \tag{21}$$

The first and fourth terms correspond to the Ornstein-Zernike approximation at equilibrium, but the exponent γ^* is expected to have the classical value:

$$\gamma^*=1 \ .$$

A^* is a function of the shear rate S:

$$A^*=a^*S^{(\gamma-1)/3\nu} \tag{22}$$

with

$$a^*=\left[\frac{16\eta}{k_BT_c}\right]^{(\gamma-1)/3\nu}\xi_0^{-1/\nu} \ . \tag{23}$$

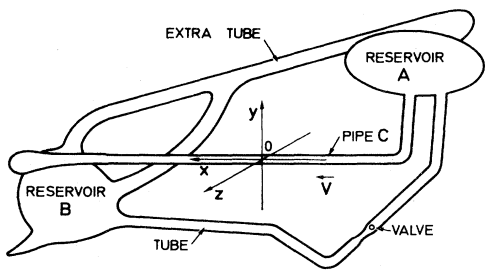

FIG. 2. Cell producing a nearly constant shear. The flow is along OX and the observation volume is close to a side wall where the shear along OY is nearly constant.

The second term is linked with the order parameter dependence. E^* depends on the shear,

$$E^*=e^*S^{1/3} \tag{24}$$

with

$$e^*=\frac{2\pi^2}{3}\left[\frac{16\eta}{k_BT_c}\right]^{1/3}\xi_0^{-1} \ . \tag{25}$$

The exponent δ^* exhibits the classical value $\delta^*=3$.

The third term describes the anisotropy of the susceptibility with respect to the flow direction. B^* is S dependent:

$$B^*=b^*S^{8/15}\propto S^{0.53} \tag{26}$$

with

$$b^*=\left[\frac{16\eta}{k_BT_c}\right]^{8/15} \ . \tag{27}$$

We point out that in contrast to the remark about (20), the critical temperature cannot be simply related to the zero of $(\chi_q^*)^{-1}$. One has to consider, at criticality $M=0$, the inverse susceptibility in the shear direction ($q_X=0$) and at very small wave vector q. With all these conditions fulfilled, a plot (linear as far as $\gamma^*=1$) of $(\chi_q^*)^{-1}$ versus T will provide T_c^*.

D. Turbidity—Transmission

Another way of gaining access to both the susceptibility and the correlation length is to measure the attenuation of the incident beam through the sample. This attenuation is due to the intense light scattering phenomenon and gives access to a somewhat "averaged" q susceptibility at the wave vector K_0 of the incident light.

Let $\mathcal{T}$ be the transmission of the incident light, and θ the turbidity. If b is the light path in the sample, then

$$\mathcal{T}=\exp(-\theta b) \ . \tag{28}$$

θ can be calculated by simply summing the scattered light intensity—i.e., the susceptibility—over a solid angle $\Omega=4\pi$:

$$\theta\propto\int_{4\pi}\chi_q d\Omega \ . \tag{29}$$

Using the equilibrium or the nonequilibrium formulation of χ_q will give different results.

1. *At equilibrium*

The formulation is well known[7]; with a linearly polarized incident beam:

$$\theta=\frac{\pi^3}{\lambda_0^4}\left[\frac{\partial n^2}{\partial M}\right]_{p,T}^2 S_n^2 C^i(1+t)t^{-\gamma}G'(\sqrt{2}K_0\xi^i)\ , \tag{30}$$

where λ_0 is the wavelength of the incident light in vacuum and n is the refractive index. S_n refers to the local field assumptions[8]: It seems that the Yvon-Vuks formulation

$$S_n=\frac{9n^2}{(n^2+2)(2n^2+1)} \tag{31}$$

is the more suitable one in binary fluids.[1,7] $(\partial n^2/\partial M)_{p,T}$ is the macroscopic derivative.

The superscript i denotes the trajectory: $i=+$, $-$, or c. In the last case, the variable t has to be changed in (30) by $(M/B_0)^{1/\beta}$, which comes from the equation (6) of the coexistence curve;

$$G'(\sqrt{2}K_0\xi^i)=G'(X_0)$$

is the integral (29) of the q-correlation function $G(X)$ as defined in (11):

$$G'(X_0)=2\sum_{i=1}^{3} c_i\{[(1+2a_i^2X_0^2)^{\mu_i}-1][1+a_i^2X_0^2(2-\mu_i)+a_i^4X_0^4(2+\mu_i+\mu_i^2)]$$
$$-2\mu_i a_i^2X_0^2(1+a_i^2X_0^2)\}[a_i^6X_0^6\mu_i(1+\mu_i)(2+\mu_i)]^{-1}\ , \tag{32}$$

where the a_i's are the same as in (11) with $\mu_i=1-b_i$.

We note that (i) θ goes to infinite, or the transmission $\mathcal{T}$ goes to zero, for $T=T_c$. This property is usually used for determining the critical point. (ii) Both C^i and ξ_0^i can be deduced from the above expressions, the other physical parameters being easily measured by standard methods.

2. *Out of equilibrium*

Unfortunately the integral (29) of the nonequilibrium susceptibility (21) cannot be calculated analytically, and other means have to be found to obtain an estimate.

a. *Numerical integration.* A solution is to numerically compute the integral for all values of the experimental parameters t^* and S, as performed by OK at $M=0$ in Ref. 2(c) for the A-C system.

b. *Approximations.* Another method consists in making some reasonable simplifications. One can note in (21) that the angular variation of the anisotropy term $(q_X^{0.4})$ is weak with respect to the last term q^2, and one can consider an average value $\langle q_x^{0.4}\rangle$ before integration. The turbidity θ^* then exhibits nearly the same functional form as at equilibrium (30) provided that the following change has been made:

$$At^{\gamma}\Longrightarrow A^*(t^*)^{\gamma^*}+E^*(M^*)^{\delta^*-1}+B^*\langle q_X^{0.4}\rangle\ . \tag{33}$$

This result calls for the following remarks.

(i) At $T_c^*(M=0)$, neither χ_q^* nor θ^* goes to infinity. The relationship (33) shows that the zero value of θ^* occurs for a reduced temperature t_a^* such that

$$t_a^*\sim-\frac{B^*}{A^*}\langle q_X^{0.4}\rangle<0\ , \tag{34}$$

where $\gamma^*=1$ has been assumed. An apparent "critical" temperature T_a can be deduced, and the apparent shift T_a-T_c can be compared to $T_c^*-T_c$:

$$T_a-T_c=(T_c^*-T_c)\left[1+\frac{1}{\nu}\left[\frac{16\eta\xi_0^3}{k_BT_c}\right]^{-0.14}\times\xi_0^{0.4}\langle q_X^{0.4}\rangle S^{-0.14}\right]\ . \tag{35}$$

With the use of typical experimental values (see Table I) and setting $\langle q_X^{0.4}\rangle\sim K_0^{0.4}$, the second bracket is always greater than 1. This apparent critical temperature change will therefore exhibit nearly the same shear dependence, between $S^{0.53}$ and $S^{0.4}$, as the actual dependence, but with a larger amplitude (see below IV E 2).

(ii) We can also compare the nonequilibrium and the equilibrium turbidities, making a temperature change t_b. From (33), we obtain (at criticality, $M^*=0$)

$$\theta(t+t_b)\sim\theta^*(t) \tag{36}$$

with $t_b=(T_b-T_c)/T_c$ deduced from

$$A(t+t_b)^{\gamma}\sim A^*(t^*)^{\gamma^*}+B^*\langle q_X^{0.4}\rangle\ . \tag{37}$$

Owing to the small difference between γ and γ^* and the relatively reduced temperature region where the condition of strong shear holds, $t_b\sim-t_a$. Although roughly in agreement with the above apparent critical temperature T_a, and showing about

TABLE I. Useful constants.

System	τ_0 (sec)	H_0 (cm)	Y_0 (cm)	S_0 (sec^{-1})	η ($10^{-2}P_0$)	ρ (g/cm^3)	c_c[d]	n[e]	$(\partial n^2/\partial\varphi)_{p,T}$	B_0	ξ_0^+ (Å)	$S_n^2 C_\varphi^+$ (10^{-23} cm^3)
A-C	13.1	7.0	0.10	1600	1.78[a]	0.87	0.470	1.52			2.45[g]	
N-H	8.7	10.4	0.115	6100	0.78[b]	0.86	0.525	1.444	0.528[f,g]	0.770[f,g]	2.65[f,g]	2.45[f,g]
		8.3	0.07	4350								
I-W		7.8	0.09	1100	2.9[c]	0.99	0.389	1.357			3.65[g]	

[a]Reference 9.
[b]Reference 10.
[c]Reference 11.
[d]Mass fraction of the first component (from Ref. 7).
[e]At T_c and for $\lambda_0=6328$ Å.
[f]Reference 14.
[g]Reference 7.

the same shear dependence as T_c^*, the temperature T_b has little to do with the actual temperature T_c^* (see below IV E 2).

c. *Determination of the β^* exponent.* Although the form of θ^* is unknown, it is nevertheless possible to infer the M dependence of χ_q. Indeed, let us define the temperature t_1^* such that the turbidity (or the transmission) at T_c^* with $M\neq 0$ is equal to the turbidity (or the transmission) at T_1^* with $M=0$:

$$\theta^*(M^*=0,t^*=t_1^*)=\theta^*(M^*\neq 0,t^*=0)\ . \tag{38}$$

This is valid also for the susceptibility (21), and then

$$A^* t_1^{*\gamma^*}=E^*(M^*)^{\delta^*-1}\ . \tag{39}$$

Using the well-known relationship[1]

$$\beta^*=\gamma^*/(\delta^*-1)\ , \tag{40}$$

the knowledge of M^* and of t_1^* as defined above allows the exponent β^* to be inferred, through

$$M^*=(A^*/E^*)^{1/(\delta^*-1)}(t_1^*)^{\beta^*}\ . \tag{41}$$

From an experimental point of view, it is not easy to determine T_c^* for each values of M. Therefore all turbidity recordings are referred to T_φ (or T_c when $M=0$), the transition temperatures at equilibrium. However, as shown in Fig. 3, the importance of the $E^*(M^*)^{\delta^*-1}$ term is such that the limiting value $\theta^*(M\neq 0,t^*=0)$ is the same at these temperatures. One can moreover estimate the importance of the approximation

$$\frac{E^*M^2}{A^* t_\varphi^*}\gg 1\ . \tag{42}$$

$t_\varphi^*<10^{-5}$ gives the condition $M\gg 10^{-3}$, when using the experimental values. This condition was always fulfilled. The relation (39) is then changed into

$$A^*\left[\frac{(T_1^*-T_c)+(T_c-T_c^*)}{T_c^*}\right]^{\gamma^*} =-A^*\left[\frac{T_c-T_\varphi}{T_c^*}\right]^{\gamma^*}+E^*(M^*)^{\delta^*-1}$$

$$\simeq E^*(M^*)^{\delta^*-1}\ , \tag{43}$$

and finally

$$M^*\simeq\left[\frac{A^*}{E^*}\right]^{1/(\delta^*-1)}\left[\frac{(T_1^*-T_c)+(T_c-T_c^*)}{T_c}\right]^{\beta^*}\ . \tag{44}$$

Here we have made $T_c^*\simeq T_c$ in the denominator, owing to the weak shift $T_c-T_c^*$. One can see that not only the experimental values of M^* and of $(T_1^*-T_c)$ are needed, but also $(T_c-T_c^*)$, which can be obtained from light scattering experiments at $M=0$, as discussed above.

The amplitude $(A^*/E^*)^{1/(\delta^*-1)}$ varies weakly with shear, since

$$\left[\frac{A^*}{E^*}\right]^{1/(\delta^*-1)}=\left[\frac{3}{2\pi^2}\left[\frac{16\eta\xi_0^3}{k_B T_c}\right]^{(\nu-1)/3\nu}\right]^{1/(\delta^*-1)} \times S^{(\nu-1)/3\nu(\delta^*-1)}\propto S^{-0.10} \tag{45}$$

using the classical value $\delta^*=3$.

E. Dynamics of return to equilibrium

When the action of shear is stopped, the system recovers its equilibrium level through a mass diffusion process. In principle, one has access to the

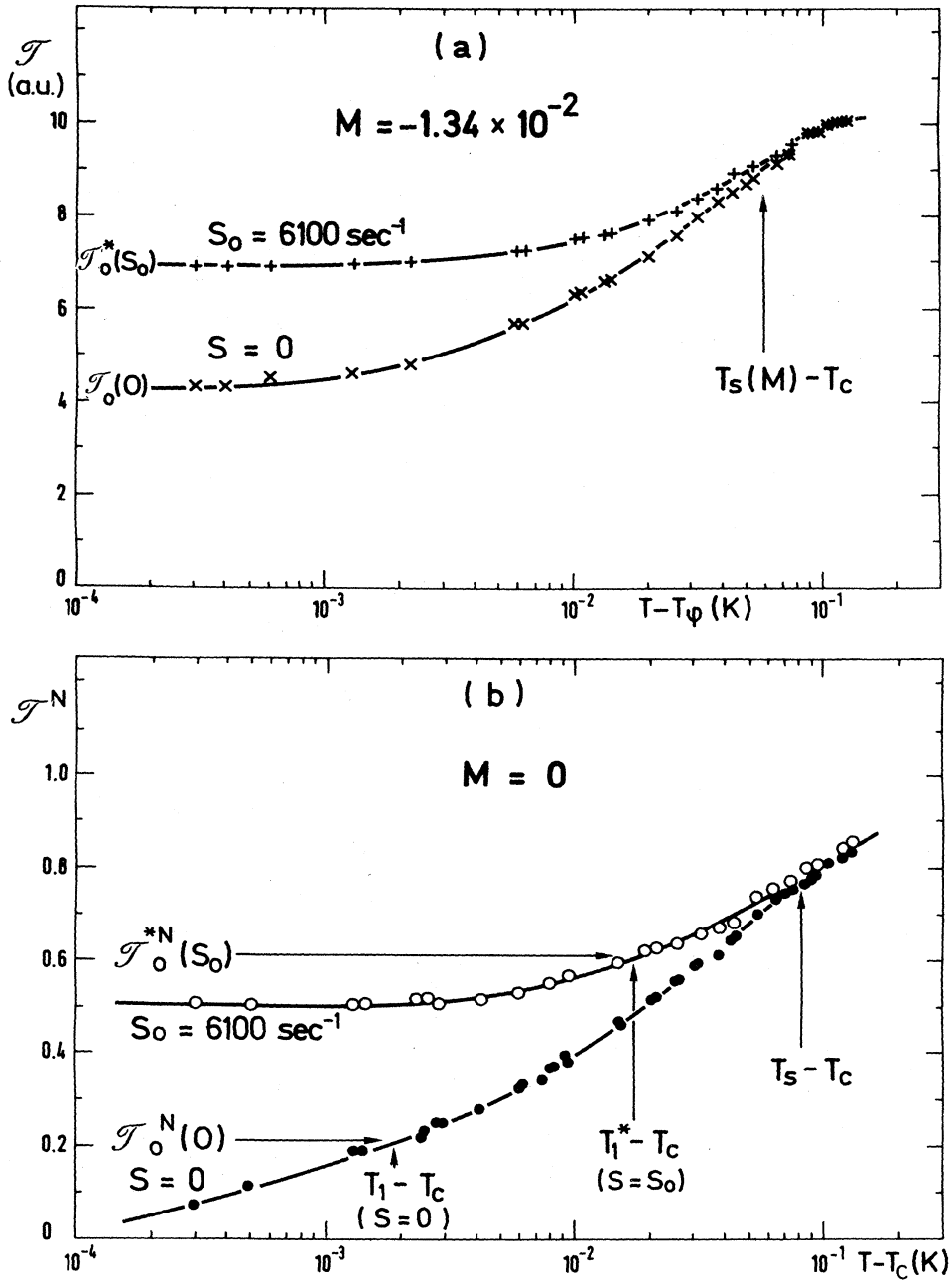

FIG. 3. (a) Transmission $\mathcal{T}$ at $M\neq 0$ vs $T-T_\varphi$, where T_φ is the phase separation temperature at equilibrium. The limiting values at $S=0[\mathcal{T}_0(0)]$ and $S\neq 0[\mathcal{T}_0^*(S_0)]$ can be deduced. $T_s(M)$ is the crossover temperature between the regions of weak and strong shear. (b) Normalized transmission $\mathcal{T}^N$ vs $T-T_c$ showing how the temperature $T_1^*-T_c$ can be deduced. T_s is the crossover temperature at criticality. $\mathcal{T}_0^{*N}$ and $\mathcal{T}_0^N$ are arbitrary.

same diffusion constants as those classically measured at equilibrium in a light scattering experiment where the time dependence of the concentration fluctuations is obtained.

It is in the flow direction where $q_x=q$ that the susceptibility (21) differs the most from its equilibrium value (20). One expects an exponential relaxation (where τ is time),

$$\chi_{q_y}(\tau)-\chi_{q_y}(\infty)\propto\exp(-\tau/\tau_q) \tag{46}$$

with the typical time τ_q is the inverse of the linewidth Γ_q. The transport coefficients are those of a system out of equilibrium at the beginning of

the process and of a system at equilibrium at the end. For simplicity, we will consider only the equilibrium case. Γ_q varies with t according to the classical relation[1,4]:

$$\tau_q^{-1}=\Gamma_q=R\frac{k_BT}{6\pi\eta\xi}q^2\Omega(q\xi)\ , \tag{47}$$

where R is a dimensionless amplitude factor of order unity and $\Omega(q\xi)=\Omega(X)$ is a function which, in its former and simpler version due to Kawasaki,[4] can be written as

$$\Omega(X)=\tfrac{3}{4}X^{-2}[1+X^2+(X^3-X^{-1})\tan^{-1}X]\ . \tag{48}$$

III. EXPERIMENTAL

Most of the experimental features have already been described in Ref. 3; we will only recall the most important points and emphasize the new aspects which enter in this work.

A. Shear flow production

The shear flow was produced in a rectangular quartz pipe (C) whose dimensions in Cartesian axes $OXYZ$ are $L_X=L=15$ cm, $a_y=a=0.3$ cm, and $b_y=b=0.5$ cm. O is the center of symmetry and OY is the vertical direction. During the run, the pipe (C) is set horizontal and the liquid flows from a reservoir A (height H_0) into another reservoir B through the pipe (C) (Fig. 2).

Two different cells have been used. The first (1) has been already described in Refs. 3(a)—3(b); the cylindrical shape of the reservoir A allowed the shear to be continuously varied with time, from a maximum value S_0 to zero. S followed the exponential variation

$$S(\tau)=S_0\exp(-\tau/\tau_0)\ . \tag{49}$$

The A-C and the N-H systems have been studied in this cell. The second cell (2) [Ref. 3(c)] has been designed for minimizing the variation of the liquid height during the run, so that the shear remains nearly constant (Fig. 2). Both the I-W and the N-H systems have been studied in this cell. Measurements are made by analyzing the scattered light or the transmission of a polarized laser beam ($\lambda_0=6328$ Å) sent along OZ, entering in $X=0$, $Y=Y_0$, near a side wall where the shear is nearly constant.

B. Determination of the shear rate

A complete description can be found in Ref. 3(b) for the A-C system, where were compared (i) the time variation of the liquid height in reservoir (A), (ii) a calculation using a Poiseuille velocity distribution in a circular pipe, and (iii) a laser doppler velocimetry determination. They are all in a relatively good agreement. Note that a calculation of the Poiseuille velocity distribution has been made in Ref. 12 for the actual rectangular pipe, and that the values of shear are in excellent agreement with the experimental value found in case iii.

We will therefore report here only the basic Poiseuille formulas for extrapolating the A-C results to other systems:

$$S_0(Y_0)=f\frac{\rho Y_0H_0}{\eta} \tag{50}$$

with

$$f=46.8\ ,$$

using the values for the A-C system reported in Table I.

As discussed in Ref. 3(c), the uncertainty on the absolute value of the shear rate is mainly due to the finite dimensions of the observed volume, and remains within 15—20 %.

For the systems A-C and I-W, the Reynolds number was lower than the critical Reynolds number ($\simeq 10^4$, but not universal), showing that turbulence was not reached. However, for the N-H system, turbulence could occur in the beginning of the run, but we have never been able to experimentally evidence it. This absence of turbulence is currently explained by the progressive entrance of the fluid into the pipe.[13]

C. Sampling—Thermal regulation

We prepared the mixtures at the critical composition, as reported in Table I. Components were of the best commercial quality, always higher than 99.5% purity. Aniline was redistilled before use, and specially treated water giving an Ohmic resistivity of 18 MΩ cm was used.

The cell (1) was sealed under vacuum at 77 K for the A-C study, as was the cell (2) for the N-H study. Owing to the presence of water in the I-W system, we pumped the cell at 0°C until some bubbles appeared, showing that the system was at the vapor pressure of the components. Then the cell was sealed.

In order to study the composition dependence of the N-H system, we sealed on the cell (1) a teflon screwtap. The cell was also pumped until some bubbles appeared, as above for the I-W system, before shutting the tap. The cells with their rotary mount were placed in water baths with thermal regulation within 0.1—0.2 mK.

The composition study of the *N-H* system needed an extra setup to measure the concentration. After each set of measurements, we removed a few cm^3 and filled a square quartz cell. This was used as a prism in a water bath with thermal regulation to measure the refractive index of the mixture by the method of the minimum deviation. From the refractive index the volume fraction was inferred within 0.1% using the Lorentz-Lorenz formula.

D. Light scattering—Turbidity

The light-scattering study was performed with the same means as already described. For the *I-W* system, the refractive index did not match the refractive index of the pipe, so particular attention was given to stray light. The transmission of the light beam was detected using calibrated photodiodes.

IV. RESULTS

We will discuss the following points: (1) critical compositions c_c and c_c^*; (2) cross-over temperature $T_s(M,S)$; (3) critical temperature T_c^*; (4) susceptibility variations with T, S, and $\vec{q}$; (5) turbidity: calibration, apparent T_c^*, M variation and exponent β^*, strong shear region in the plane (M,T); (6) dynamics of return to equilibrium; (7) susceptibility and correlation length at equilibrium on the critical isochore above and below T_c, and on the critical isotherm.

A. Critical compositions c_c and c_c^* (*N-H* system)

Although, in principle, the action of shear does not modify the composition and/or the critical concentration, we wanted to check this point.

For the turbidity behavior at equilibrium, we make use of the remarks on θ made in II D 1 where it was pointed out that the zero value of the transmission coincides with the critical point. Therefore the asymptotical value of $\mathcal{T}$ when $T \to T_\varphi$, noted $\mathcal{T}_0$, will go to zero only for $c = c_c$. A plot of $\mathcal{T}_0$ vs c will thus enable c_c to be determined.

Out of equilibrium, the anisotropy term in χ^* [see (21)] prevents θ^* from diverging at t_c^*, but θ^* presents a maximum for c_c^*. The plot of the limiting transmission $\mathcal{T}_0^*$ for $T = T_\varphi$, vs c, will therefore exhibit a minimum for $c = c_c^*$.

For calibration reasons explained below in IV E 1, we have divided all the $\mathcal{T}_0$ and $\mathcal{T}_0^*$ values by the transmissions $\mathcal{T}_{0.1}$ or $\mathcal{T}_{0.1}^*$ at the same concentration, but measured at 0.1 K above T_φ. This fact of course does not change the location of the minima. The ratios $\mathcal{T}_0/\mathcal{T}_{0.1}$ and $\mathcal{T}_0^*/\mathcal{T}_{0.1}^*$ have been plotted in Fig. 4. Only the experiments performed at the highest and lowest shears have been reported, the other shears giving rise to a quite similar behavior. The full line in Fig. 4 is the ratio $\mathcal{T}_0/\mathcal{T}_{0.1}$ calculated according to the formulation of $\mathcal{T}_{0.1}$ elaborated below in IV E 1. The values of $\mathcal{T}_0$ on the coexistence curve have been calculated from θ as written in (30) where the variable t was changed into $(M/B_0)^{1/\beta}$. We have used the values of Table I.

This function fits the data well at $S=0$ provided that $c_c = 0.526$ mass fraction (a value in agreement with that already published,[7,14] 0.525). However, the most important result is that the minima obtained with experiments under shear or at equilibrium coincide (Fig. 4):

$$c_c^* = c_c = 0.526 \,. \tag{51}$$

B. Crossover temperature T_s: Variation with M and S

The transmission shows a change of behavior when $T < T_s$ (Fig 3). It is easy to determine with the recordings themselves a temperature T_s at which an effect is visible within the experimental sensitivity, whose order of magnitude is 2%.

1. M dependence

For the *N-H* system in the cell no. 1, the temperatures T_S have been reported for various values of M and plotted in Fig. 1 , where only one shear has been reported, the other shears giving the same kind of results.

Since all recordings have been obtained as a function of $T - T_\varphi$, we had to add to the experimentally determined value $T_S - T_\varphi$, the quantity

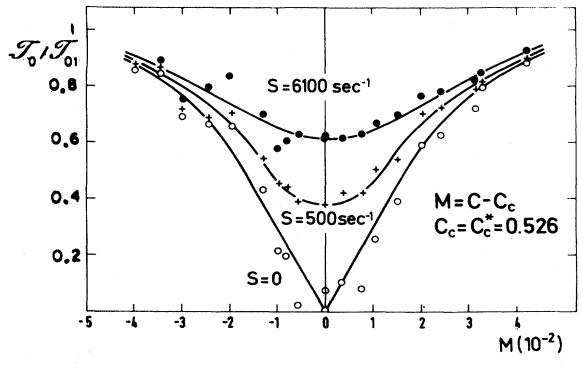

FIG. 4. Determination of the critical mass concentration with (c_c^*) or without (c_c) shear. We have used the minimum of transmissions ratios $\mathcal{T}_0/\mathcal{T}_{0.1}$. $\mathcal{T}_{0.1}$ is the transmission at 0.1 K from the phase-separation temperature T_φ, and $\mathcal{T}_0$ is the transmission at T_φ. The full line for $S=0$ corresponds to the formula used in IV E 1.

$$T_\varphi - T_c = -T_c(M/B_0)^{1/\beta} \tag{52}$$

with B_0 from Table I, to obtain $[T_s(M)-T_c]$.

The solid line in Fig. (1) is the best fit to Eq. (53) derived from (9):

$$M = B_s \left[\frac{(T_s - T_c) - [T_s(M) - T_c]}{T_c} \right]^{\omega} . \tag{53}$$

The 3 quantities B_S, $(T_S - T_c)$, and ω are the adjustable parameters. We have found for the highest shear:

$$S = 6100 \text{ sec}^{-1} \begin{cases} \omega = 0.6 \pm 0.1 \\ B_S = 5 \pm 4 \\ T_S - T_c = (7.4 \pm 0.5) \times 10^{-2} \text{ K} . \end{cases}$$

Note the agreement of ω with expected value $\frac{1}{2}$. We have also imposed ω to $\frac{1}{2}$ in order to increase the accuracy on B_S:

$$S = 6100 \text{ sec}^{-1} \begin{cases} \omega = \frac{1}{2} \text{ imposed} \\ B_s = 2.15 \pm 0.04 \\ T_s - T_c = (7.0 \pm 0.3) \times 10^{-2} \text{ K} . \end{cases}$$

It is interesting to compare these amplitudes with those calculated from (4) and (9), using the numerical values of Table I:

$$B_S^{\text{theor}} = 2.03 ,$$

in excellent agreement with the above experimental value, and

$$(T_s - T_c)^{\text{theor}} = 0.112 \text{ K} ,$$

which is bigger, but of the same order of magnitude. That both the exponent ω and the amplitude B_S agree well with the expectations, and that only $T_s - T_c$ disagree, is presumably due to the arbitrary, but permanent, criterion we have chosen to determine $T_s(M)$.

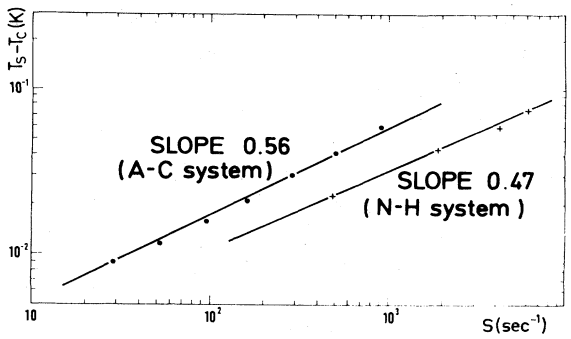

FIG. 5. Crossover temperature variation with shear from transmission data. The straight line corresponds to a power law. The expected exponent is $\frac{1}{3}\nu = 0.53$.

2. *S dependence*

We follow the same analysis as above, but at the critically $M=0$, using (i) transmission data in *N-H* and *A-C* at different shear rates (cell no. 1), and (ii) transmission data in *N-H* and *I-W* at constant shear rate (cell no. 2).

All data concerning various shear rates are reported in Fig. (5). The expected variation (4) is visible. More particularly, if one considers (54) which comes from (4)

$$T_s - T_c = \Sigma_0 S^{\sigma_0} \tag{54}$$

with Σ_0 and σ_0 as unknown parameters, one finds

$$\begin{array}{l} \textit{A-C} \\ S \text{ range: } 30-900 \text{ sec}^{-1} \end{array} \begin{cases} \sigma_0 = 0.56 \pm 0.03 \\ \Sigma_0 = (1.3 \pm 0.2) \times 10^{-3} \text{ cgs units} \\ \Sigma_0 = (1.5 \pm 0.1) \times 10^{-3} \text{ cgs unit with } \sigma_0 = 0.53 \text{ imposed} . \end{cases}$$

The value of the amplitude Σ_0 has to be compared with another value in the same system, obtained by analyzing the scattered intensity at 2 angles [Ref. 3(b)], $\Sigma_0 \simeq 2.3 \times 10^{-3}$ cgs units. These values are comparable when one accounts for the uncertainties of these measurements [see Fig. 6 of Ref. 3(b)].

Using the numerical values of Table I, we can calculate the theoretical amplitude,

$$\Sigma_0^{\text{theor}} = 1.58 \times 10^{-3} \text{ cgs units} ,$$

which is in close agreement with the experimental value.

For the *N-H* system, studied at various shear rates (Fig. 5), we find

$$\begin{array}{l} \textit{N-H} \\ S \text{ range: } 500-6000 \text{ sec}^{-1} \end{array} \begin{cases} \sigma_0 = 0.47 \pm 0.05 \\ \Sigma_0 = (7.9 \pm 0.4) \times 10^{-4} \text{ cgs units} . \end{cases}$$

The last value was obtained with $\sigma_0 = 0.53$ imposed. If one considers the *N-H* transmission data [Fig. 6(b)] in the cell no. 2 (constant shear), we find

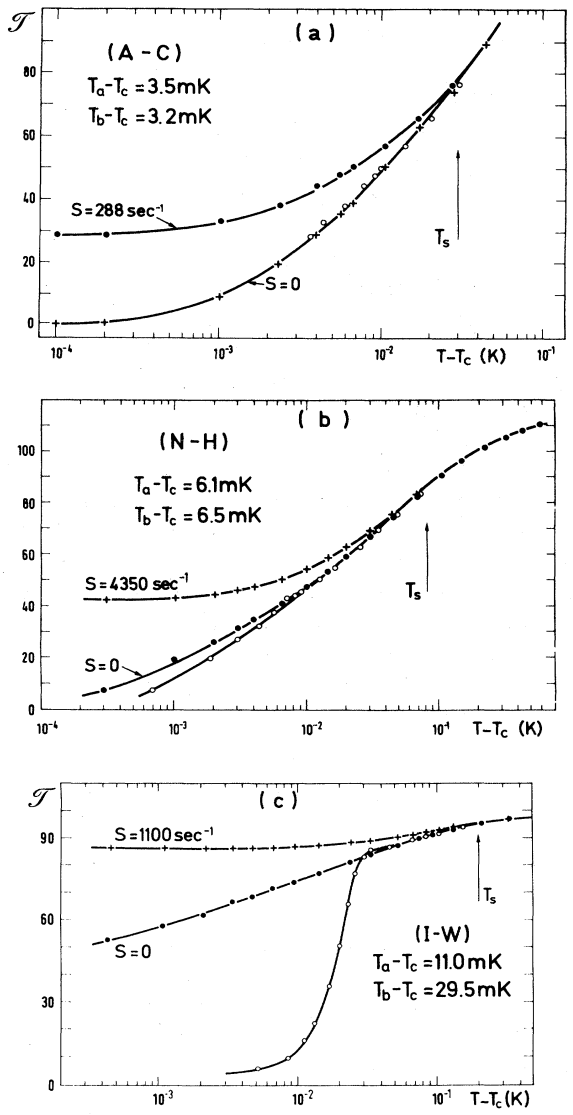

FIG. 6. Transmission variation $\mathcal{T}$ vs $T-T_c$ for $S=0$ (full circles) and $S\neq 0$ (crosses). The open circles correspond to the transmission $\mathcal{T}(S\neq 0)$ translated by the quantity (T_a-T_c). T_b is the temperature at which $\mathcal{T}(S\neq 0)$ goes to zero. (a) *A-C* system $T_b\simeq T_a$, (b) *N-H* system $T_b\simeq T_a$, (c) *I-W* system: Due to the large transmission even close to T_c, T_a has been determined by the value $\mathcal{T}(S\neq 0)=0.5$ which corresponds to the value of $\mathcal{T}(S=0)$ within 0.2 mK from T_c.

$$\left.\begin{array}{l} N\text{-}H \\ S=4350\ \text{sec}^{-1} \end{array}\right\} \Sigma_0=(9.4\pm 2.4)\times 10^{-4}\ \text{cgs units}\ .$$

These 2 results can be compared to the theory using values of Table I:

$$\Sigma_0^{\text{theor}}=11.2\times 10^{-4}\ \text{cgs}\ .$$

Finally, the *I-W* mixture transmission of Fig. (6) allows also an amplitude to be determined,

$$\left.\begin{array}{l} I\text{-}W \\ S=1100\ \text{sec}^{-1} \end{array}\right\} \Sigma_0=(4\pm 1)\times 10^{-3}\ \text{cgs}\ ,$$

which is to be compared with the expected amplitude, calculated with the values of Table I:

$$\Sigma_0^{\text{theor}}=3.75\times 10^{-3}\ \text{cgs}\ .$$

Reasonable agreement is therefore found, both for exponent σ_0 and amplitude Σ_0.

C. Critical temperature T_c^*

As noted above in II D 2 b, the transmission measurements are of no use for determining T_c^*; however T_c^* can be characterized by the divergence of the scattered light in the flow direction at very small wave vector q (see II C 2). More exactly, the inverse susceptibility

$$\chi_q^{-1}=A^*\left[\frac{T-T_c^*}{T_c^*}\right]\gamma^*+q^2\simeq A^*\left[\frac{T-T_c}{T_c}\right]\gamma^*\ , \tag{55}$$

plotted versus T in linear coordinates, must be extrapolated to zero for $T=T_c^*$.

This has been done for the *N-H* and *I-W* systems in Fig. 7, studied at constant shear rate (cell no. 2). There is a small, but noticeable, change in the critical temperature.

With A^* free and $\gamma^*=1$ imposed, in accordance with the results shown in Fig. 7, the fit of the data to the exact formula (55) gives the shifts in T_c:

$$\left.\begin{array}{l} N\text{-}H \\ S=4350\ \text{sec}^{-1} \\ q=6600\ \text{cm}^{-1} \end{array}\right\} T_c^*-T_c=(1.8\pm 1)\times 10^{-3}\ \text{K}\ ,$$

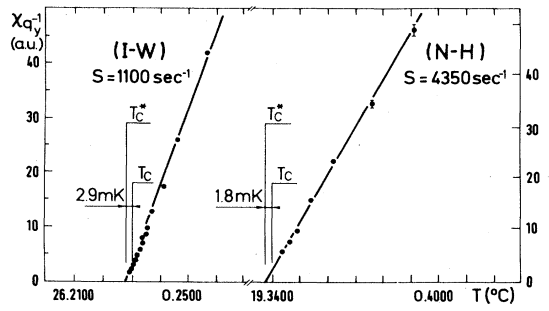

FIG. 7. Determination of the critical temperature under shear T_c^* from the zero of the inverse susceptibility in the shear direction ($\chi_{q_y}^{-1}$). T_c is the critical temperature at equilibrium. The linear variation of $\chi_{q_y}^{-1}$, moreover, shows that the mean-field approach is relevant.

$$\begin{matrix} I\text{-}W \\ S=1100\ \text{sec}^{-1} \\ q=6600\ \text{cm}^{-1} \end{matrix}\left\{ T_c^*-T_c=(2.9\pm0.2)\times10^{-3}\ \text{K}\ . \right.$$

These amplitudes can be compared to the expected values according to (7). More precisely, the universal constant v can be estimated:

$$N\text{-}H:\ v=(1.9\pm1)\times10^{-2}\ ,$$

$$I\text{-}W:\ v=(1.9\pm0.13)\times10^{-2}\ .$$

There is good agreement between both experimental values, but they are about 4 times lower than the expected value

$$v^{\text{theor}}=8.32\times10^{-2}\ .$$

However, this amplitude is sensitive to the kind of flow[2] and has been calculated only for a rigorously constant shear rate.

Anyway, assuming for the kind of flow studied here

$$v\simeq2\times10^{-2}\ ,$$

we are able to predict the T_c shift for the *A-C* system. Using the values of Table I, we find

$$T_c^*-T_c\simeq3\times10^{-5}S^{1/3\nu}\ . \tag{56}$$

This value is significantly different from that

$$T_a-T_c=1.8\times10^{-5}S^{1/3\nu} \tag{57}$$

coming from the transmission measurements and which was used in Ref. 3 to interpret the susceptibility data. In the following, we will therefore reanalyze the *A-C* data for which this T_c shift has an influence.

D. Susceptibility variations with T, S, and q

This study was performed at criticality $M=0$.

1. *T variations of χ_q at q,s fixed: Exponent γ^**

We will consider the 2 limiting cases $q_x=0$ and $q_x=q$. According to the expected χ_q variation (21), with $M=0$, the interest of experiments performed at very small q is obvious for removing the classical q^2 dependence.

a. *$q_x=0$.* We are concerned with the *N-H* and *I-W* systems at constant shear rate (cell no. 2). Figure 7 already showed that in linear coordinates, χ_q^{-1} vs T exhibited for both systems a linear variation, demonstrating the classical value of γ^*.

A fit to (55) with A^*, T_c^*, and γ^* free allows the following values to be obtained:

$$\begin{matrix} N\text{-}H \\ S=4350\ \text{sec}^{-1} \\ q=6600\ \text{cm}^{-1} \end{matrix}\left\{ \begin{matrix} \gamma^*=0.98\pm0.09 \\ [T_c^*-T_c=(1.5\pm1.5)\times10^{-3}\ \text{K}]\ , \end{matrix} \right.$$

$$\begin{matrix} I\text{-}W \\ S=1100\ \text{sec}^{-1} \\ q=6600\ \text{cm}^{-1} \end{matrix}\left\{ \begin{matrix} \gamma^*=0.92\pm0.03 \\ [T_c^*-T_c=(1.9\pm0.2)\times10^{-3}K]\ . \end{matrix} \right.$$

The classical value $\gamma^*\simeq1$ is obtained. χ_q versus $T-T_c^*$ has been reported in Fig. (8) for the 2 regimes of strong and weak shears, where γ^* exhibits the classical value 1 or the usual value 1.24. The value of $T_c-T_c^*=2.9$ mK corresponds to a fit with $\gamma^*=1$ imposed (see above IV C).

b. *$q_x=q$.* We will only discuss the data from the *A-C* system. Whether the T_c shift (56) or that (57) estimated from transmission measurements is used very much changes the behavior [see Fig. 9(a) and 9(b)]. The mean-field behavior which was visible using the shift (57) is quite normal, since, from the definition of T_a (34) and neglecting the q^2 term:

$$\chi_q^{-1}=A^*\left[\frac{T-T_a}{T_c}\right]+b^*S^{8/15}(q^{0.4}-\langle q_x^{0.4}\rangle)$$

$$\simeq A^*\left[\frac{T-T_a}{T_c}\right]\ . \tag{58}$$

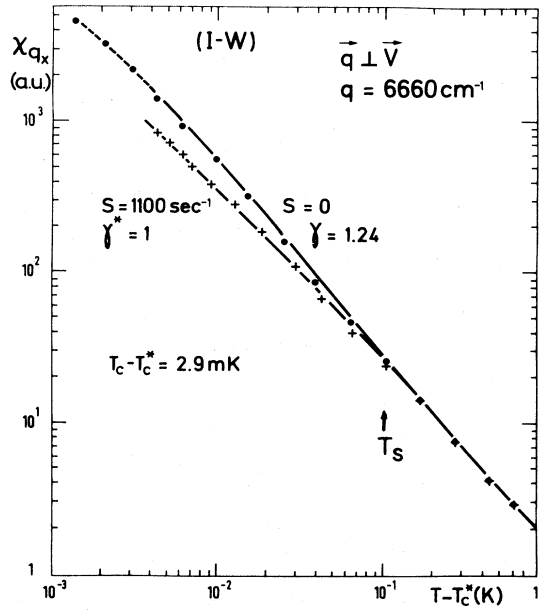

FIG. 8. Variations of the susceptibility in the shear direction vs $T-T_c^*$ showing the regular behavior when $S=0$ or $S\neq0$ and $T>T_s$, and the mean-field behavior when $S\neq0$ and $T<T_s$.

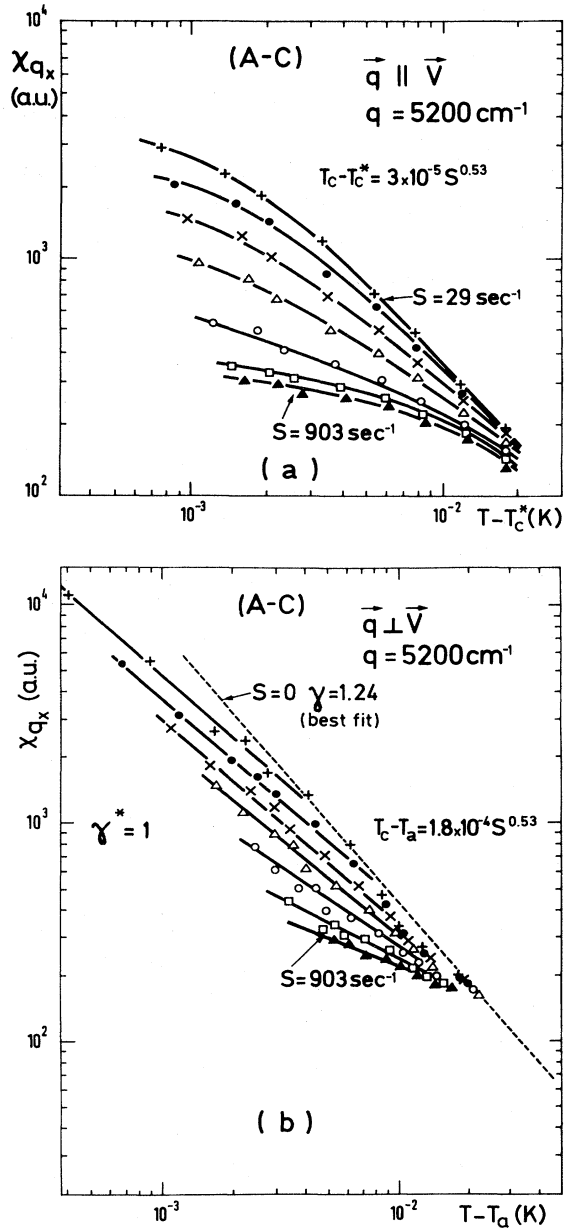

FIG. 9. Variations of the susceptibility in the flow direction, for the *A-C* system, vs (a) $T-T_c^*$, using the formula (56) which comes from results obtained in the (*N-H*) and (*I-W*) mixtures. (b) $T-T_a$, where T_a is the apparent critical temperature [formula (57)] obtained by transmission measurements. The following shears have been studied: (△) 903; (□) 510; (○) 288; (△) 163; (×) 92; (●) 52; (+) 29 sec^{-1}.

One can see that the anisotropy term is reduced when compared to the temperature term. It is only at the strongest shears, when $b^*S^{8/15}$ becomes important, that a curvature in a double-logarithm plot of χ_q vs $T-T_a$ becomes visible [Fig. 9(b)].

2. *S-variations of χ_q at T and q fixed*

Using the *A-C* data of Fig. 9(a) with the "right" T_c shift (56), it is easy to consider the values of $\chi_q(q_x=q)$ at constant temperature. We wanted to make visible the shear dependence of B^*, so only the data very close to T_c^* has to be retained. From (21),

$$\chi_q^{-1}=A^*(t^*)^{\gamma^*}+b^*S^{8/15}q^{0.4}+q^2\simeq b^*q^{0.4}S^{8/15}\ . \tag{59}$$

In Fig. 10 these data have been reported and fitted to the variation:

$$\chi_q^{-1}=X_1+X_2S^{\sigma_2}\ , \tag{60}$$

where X_1, X_2, and σ_2 are adjustable parameters. We have found

$$\sigma_2=0.6\pm0.1\ ,$$

i.e., a value in agreement with the expected value $\frac{8}{15}\simeq0.53$. This result is interesting, since in Ref. 3(b) where the *A-C* data were analyzed, a value $\sigma_2\sim1$ was found due to the use of T_a instead of T_c^*.

3. *q variations of χ_q at T and S fixed*

According to (21), the variation (61) is expected:

$$\chi_q^{-1}=X_1[X_2+X_3q_X^{\pi}+q^2]\ . \tag{61}$$

Here $X_2=A^*t^*$, $X_3=b^*S^{8/15}$, and $\pi=0.4$. X_1 is an arbitrary factor. Obviously only the experiments performed at the closest temperatures to T_c (X_2 minimum), at the highest shears (X_3 maximum), and for the smallest q (q^2 minimum) will render the exponent of q_X detectable.

The conclusions of Ref. 3(b) concerning the *A-C* mixture remain valid since the temperature term X_1 was left free in the analysis, together with X_2, X_3,

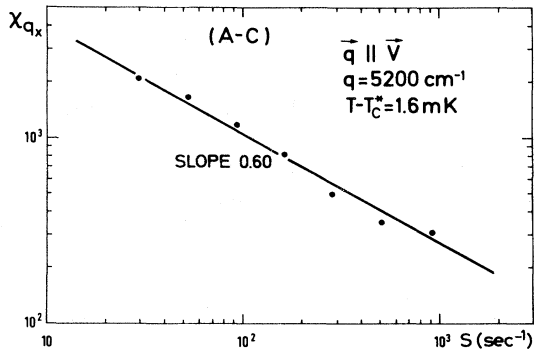

FIG. 10. Variations of the susceptibility in the flow direction vs shear, close to T_c^*, showing a power-law dependence with an exponent whose expected value is 0.53.

and π. The results, with either $q=cst$ and q_X varying or $q_X=q$, q varying, gave the same result, in agreement with the theoretically expected value 0.40:

$$\left.\begin{array}{l} A\text{-}C \\ S \text{ range: } 30\text{—}900 \text{ sec}^{-1} \end{array}\right\} \pi=0.40\pm0.05 .$$

Only the *I-W* system has been investigated at constant shear rate, in the configuration $q_X=q$, and q varying. The data recorded within 3 mK and 10 mK from T_c have been reported in Fig. (11). An exponent π, with value

$$\pi=0.55\pm0.05 ,$$

has been found. This somewhat high value is presumably due to the terms in $q^{0.4}$ and q^2 which combine in the q range investigated, making an effective exponent slightly larger than 0.4.

E. Turbidity

1. *Calibration of transmission data*

For practical reasons, the transmission recordings were not performed at temperature differences $T-T_\varphi$ greater than about 0.2 K. Since all recordings needed to be carefully recalibrated, we choose as a standard the transmission $\mathcal{T}_{0.1}$ at 0.1 K from T_φ. Indeed, at this temperature the effect of the shear is negligible, so $\mathcal{T}^*_{0.1}=\mathcal{T}_{0.1}$, and the influence of the concentration is generally much lower than that of the temperature, making $\mathcal{T}_{0.1}$ weakly dependent on M.

The theoretical value $\mathcal{T}_{0.1}$ is unknown, since the amplitudes of ξ and χ are defined only on special trajectories such as the critical isochore or the critical isotherm. Nevertheless, in the M range studied,

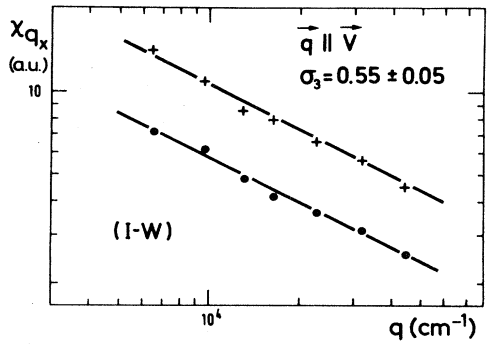

FIG. 11. Susceptibility in the flow direction vs q, showing a power law with exponent π, whose theoretical value is 0.40. Data have been obtained at $T-T_c=3$ mK (+) and $T-T_c=10$ mK (●).

the condition

$$0.1 \gg T_c-T_\varphi \tag{62}$$

is always fulfilled, and this fact allows some approximations to be made.

a. *Susceptibility.* If one considers the formulation of the free energy ϕ (Ref. 1) and the definition of the susceptibility

$$\chi^{-1}=\frac{\partial\mu}{\partial M}=\frac{\partial^2\phi}{\partial M^2} , \tag{63}$$

one obtains

$$\chi^{-1}=\frac{t^\gamma}{C_0}+\delta D_0 M^{\delta-1} . \tag{64}$$

The amplitudes C_0 and D_0 are known only on special trajectories, such as $t>0$, $M=0$ ($C_0=C^+$), and $t=0$ ($D_0=D$). We will simply assume that $C_0=C^+$ and $D_0=D$. In this case, and using the universal amplitude factor $R_\chi^+=C^+DB^{\delta-1}$ whose theoretical value is 1.7 (Ref. 15), we can write (64) as

$$\chi^{-1}\simeq\frac{1}{C^+}[t^\gamma+\delta R_\chi^+(M/B_0)^{\delta-1}] . \tag{65}$$

b. *Correlation length.* We follow the same kind of arguments and assume

$$\xi(t,M)\simeq\xi_0^+\left[t+\left|\frac{M}{B_0}\right|^{1/\beta}\right]^{-\nu} . \tag{66}$$

This relationship remains valid for $M=0$. For $t=0$, we have to change the amplitude ξ_0^+ by another (ξ_0') including ξ_0^c. With the universal ratio,[16]

$$Q_2=\frac{C^+}{C_c}\left[\frac{\xi_0^c}{\xi_0^+}\right]^{2-\eta}=1.21 ,$$

we obtain

$$\xi_0'=\xi_0^+\left[\frac{Q_2}{\delta R_\chi^+}\right]^{1/(2-\eta)}\simeq1.0 \text{ Å} ,$$

using $\xi_0^+=2.65$ Å from Table I. The relation (66) is therefore only an approximation and is valid in the range where the condition (62) holds.

Putting the expressions (65) and (66) in the calculation of θ through (29), one obtains the same expression as (30), but where the following changes have to be made:

$$t^{-\gamma}\rightarrow\left[t_{0.1}^\gamma+\delta R_\chi^+\left[\frac{M}{B_0}\right]^{\delta-1}\right]^{-1} , \tag{67}$$

$$\xi^i\rightarrow\xi_0^+\left[t_{0.1}+\left[\frac{M}{B_0}\right]^{1/\beta}\right]^{-\nu} \tag{68}$$

with $t_{0.1}=0.1/T_c$.

A check of this formulation has been performed in Fig. (4) where the ratio of the transmission at T_φ (i.e., $\mathcal{T}_0$) to the transmission at $T_\varphi + 0.1$ K (i.e., $\mathcal{T}_{0.1}$) have been plotted in function of M.

2. *Apparent T_c^**

As stressed in II D 2 b, transmission measurements may lead to an apparent critical temperature T_a if the same criterion as at equilibrium is applied for systems under shear.

In Fig. 6 the data at $S=288$ sec^{-1} from Ref. 3(b) have been reported for the *A-C* system, together with the measurements performed in the *N-H* and *I-W* mixtures. Let us compare the apparent shift $T_a - T_c$ with the one predicted by OK $(T_c^* - T_c)_{\text{theor}}$:

$$\begin{array}{ll} A\text{-}C & \\ S \text{ range } 30\text{—}900 \text{ sec}^{-1} & \left\{ \dfrac{T_a - T_c}{(T_c^* - T_c)_{\text{theor}}} = 1.4 \right. , \\ N\text{-}H & \\ S = 4350 \text{ sec}^{-1} & \left\{ \dfrac{T_a - T_c}{(T_c^* - T_c)_{\text{theor}}} = 0.8 \right. , \\ I\text{-}W & \\ S = 1100 \text{ sec}^{-1} & \left\{ \dfrac{T_a - T_c}{(T_c^* - T_c)_{\text{theor}}} = 0.9 \right. \end{array}$$

(T_a was determined in this weakly opalescent system by the transmission value at 0.2 mK from T_c). The fact that this ratio is of order unity is presumably a mere coincidence.

We can also determine T_b such as $\mathcal{T}(T + T_b - T_c) \simeq \mathcal{T}^*(T - T_c)$ (see above II D 2 b and Fig. 6). The above approximation is well supported by the *A-C* system Ref. 3; for the other mixtures, the comparison with $(T_c^* - T_c)_{\text{theor}}$ gives also ratios of order unity:

$$\begin{array}{ll} A\text{-}C & \\ S \text{ range } 30\text{—}900 \text{ sec}^{-1} & \left\{ \dfrac{T_b - T_c}{(T_c^* - T_c)} = 1.4 \right. , \\ N\text{-}H & \\ S = 4350 \text{ sec}^{-1} & \left\{ \dfrac{T_b - T_c}{(T_c^* - T_c)_{\text{theor}}} = 0.85 \right. , \\ I\text{-}W & \\ S = 1100 \text{ sec}^{-1} & \left\{ \dfrac{T_b - T_c}{(T_c^* - T_c)_{\text{theor}}} = 2.4 \right. . \end{array}$$

3. *M variation*

Transmission recordings for 20 different compositions have been recorded with the *N-H* system, using the cell no. 1 where the shear was continuously varying with time. Typical recordings are shown in Fig. 3. As discussed above in (II D 2 c), the limiting value $\mathcal{T}_0^*(M \neq 0)$ can be compared to that at $M=0$ in order to determine the quantity $T_1^* - T_c$. The plot of M vs $[(T_1^* - T_c) + (T_c - T_c^*)]$ is expected to be a straight line in a double-logarithmic plot and allows, according to (44), the exponent β^* to be determined.

In Figs. 12(a)—12(d) the data for 4 shears ranging from 500 to 6100 sec^{-1} have been reported. The values of $T_c - T_c^*$ have been deduced from the results of IV C:

$$(N\text{-}H) \quad T_c^* - T_c = (2.1 \pm 1.2) \times 10^{-5} S^{0.53} . \qquad (69)$$

The large uncertainty on this coefficient has nevertheless only a weak influence on the results, $T_c^* - T_c$ being always small compared to $T_1^* - T_c$.

Owing to the method itself, data very close to T_c (within a few mK) are useless and have been discarded.

In order to check this method, we have also analyzed the transmission at equilibrium. In Fig. 12(e) are reported the data, which are in agreement with the equilibrium exponent $\beta = 0.325$, whereas all values obtained at $S \neq 0$ agree with the classical value $\beta^* = \frac{1}{2}$.

According to (44), one can fit the data to

$$M^* = H^* \left[\frac{T_1^* - T_c^*}{T_c} \right]^{\beta^*} \qquad (70)$$

with H^* and β^* as adjustable parameters. One obtains a value $\beta^* = \frac{1}{2}$ within 3—5 %, and an amplitude $H^* = 2$—2.3 close to the theoretical values 1.6—2 in the S range 6100—500 sec^{-1}. Details of the fits are given in Table II. According to (45), H^* should vary with $S^{-0.10}$; the values found here are in agreement with $S^{-0.05}$, but the exponent accuracy is poor.

4. *Strong shear region in the plane (M,T)*

It is possible to deduce the coexistence curve under shear, which obeys Eq. (5), or, with respect to T_c, Eq. (71):

$$M = B_0^* \left[\frac{(T_c^* - T_c) + (T_c - T_\varphi^*)}{T_c^*} \right]^{\beta^*} . \qquad (71)$$

In this formula, B_0^*, $T_c - T_c^*$, and β^* are unknown. However:

(i) The value of exponent β^* has been shown to be $\frac{1}{2}$ (see IV E 3).

(ii) The value of $T_c - T_c^*$ has been determined; for instance, with $S = 6100$ sec^{-1}, $T_c - T_c^* = (2.21 \pm 1.2) \times 10^{-3}$ K when one applies the results of IV C and the relation (69).

(iii) B_0^* can be determined if one notices that the intersection of the crossover function with the coexistence curve at equilibrium must coincide with the intersection with the coexistence curve out of equilibrium (see Fig. 1). For the shear rate $S = 6100$

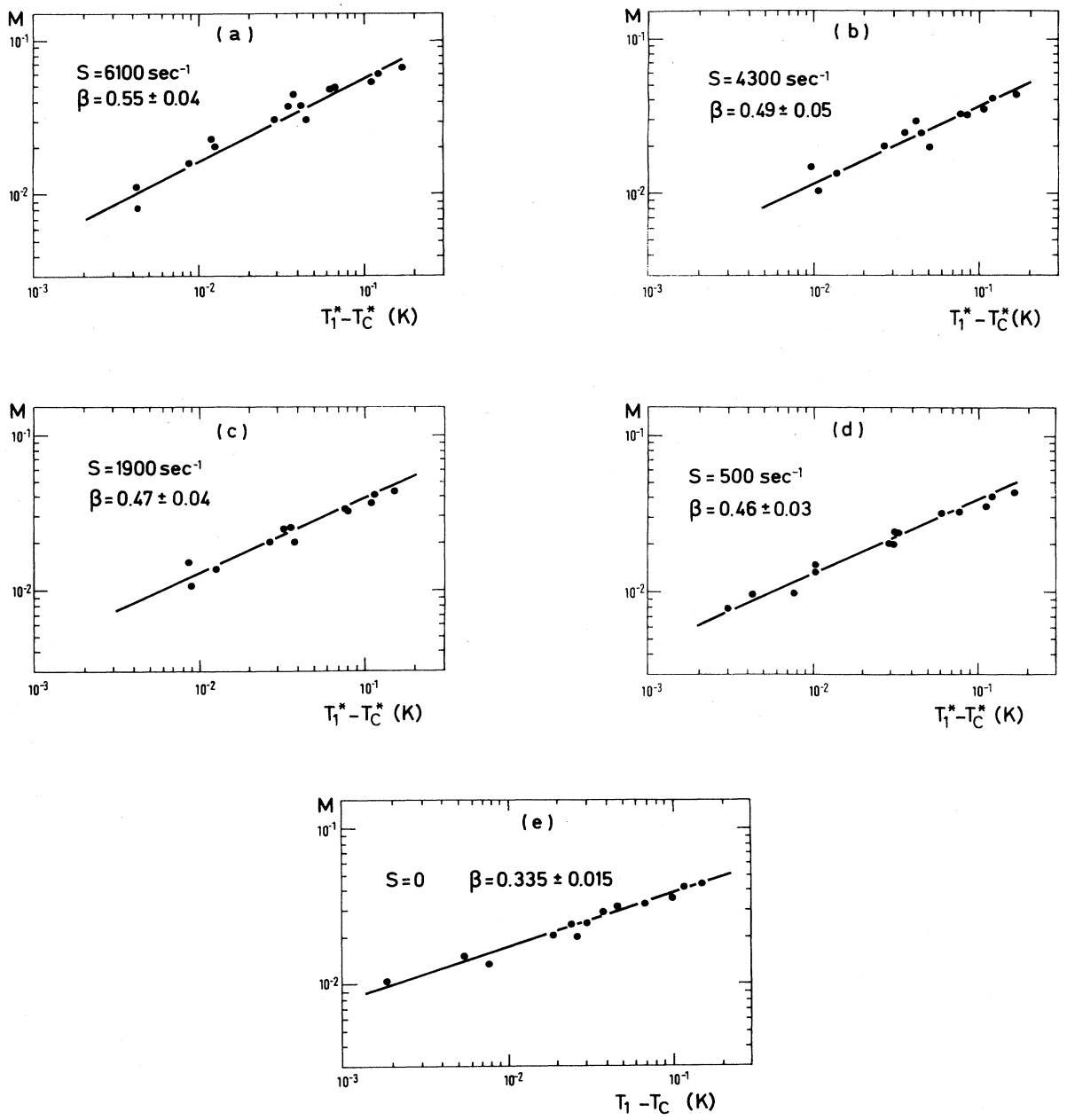

FIG. 12. (a)—(e) Variations of the order parameter M vs the temperature difference $T_1^* - T_c^*$ (see text), allowing the exponent β^* to be measured. Its value is expected to be $\frac{1}{2}$ when $S \neq 0$, and 0.325 when $S=0$.

sec^{-1}, one finds

$$B_0^* \simeq 3.9 .$$

The calculation of the uncertainty is not easy, but we estimate it to within 20—30 %.

Therefore the region of strong shear, delimited by the cross-over temperature $T_s(M)$ and the phase-separation temperature $T_\varphi(M)$, can be determined. It has been drawn for $S=6100$ sec^{-1} in Fig. 1 (hatched region).

It is interesting to note that the phase separation shift due to the shear is maximum not at criticality, but for values of M of order 0.02, where it is about three times larger than at $M=0$.

F. Dynamics of return to equilibrium

In the I-W mixture at criticality we have studied how a system perturbed by a shear recovers equili-

TABLE II. Fit of M vs $T_1 - T_c^*$ in the N-H system according to $M = H^*(T_1 - T_c^*/T_c)^{\beta^*}$ with H^* and β^* as adjustable parameters. The theoretical value is $\beta^* = \frac{1}{2}$ when $S \neq 0$, and 0.325 when $S = 0$. H^* is expected to be about 2 when $S \neq 0$. The quantities in brackets have been imposed in the fit.

S (sec^{-1})	β^*	H^*
6100	0.55 ±0.04	2.8 ±0.7
	($\frac{1}{2}$)	2.00±0.08
4300	0.49 ±0.05	1.9 ±0.7
	($\frac{1}{2}$)	2.02±0.08
1900	0.47 ±0.04	1.7 ±0.6
	($\frac{1}{2}$)	2.10±0.09
500	0.46 ±0.03	1.6 ±0.4
	($\frac{1}{2}$)	2.27±0.10
0	0.335±0.015	0.56±0.09
	(0.325)	0.50±0.01

brium when this shear is suddenly stopped.

From the susceptibility under shear (Eq. (21), it is clear that the intensity scattered in the X direction ($q_X = q$) will give rise to the larger effect. In Fig. 13(a) are shown typical recordings. The scattered intensity, once corrected for the transmission, is seen to exhibit the expected experimental behavior (see II E) with characteristic time τ_q [Fig. 13(b)]. This typical time, determined for 3 wave vectors $q = 32\,500$, 16 500, and 6660 cm^{-1} and in the temperature range 5×10^{-4} K to 3×10^{-2} K, has been reported in Fig. (14) versus $T - T_c$. The full line is Γ_q^{-1} from formula (47), using the numerical values of Table I, and letting free the amplitude ratio R. The values found are very small and depend on the value of q, whereas the temperature variation agrees relatively well with the formulation of τ_q. The reason why very low values of R have been obtained is certainly related to the simplification made when we considered the system to be at equilibrium.

G. Susceptibility and correlation length at equilibrium: Amplitude combinations

We have also analyzed the turbidity data of the N-H system when $S = 0$ and M varying. These data are reported in Fig. 15, together with others from Ref. 14, where can be found the numerical values.

1. *Critical isochore above T_c*

The transmission recording for $M = 0$ has been analyzed according to formula (30), and gives

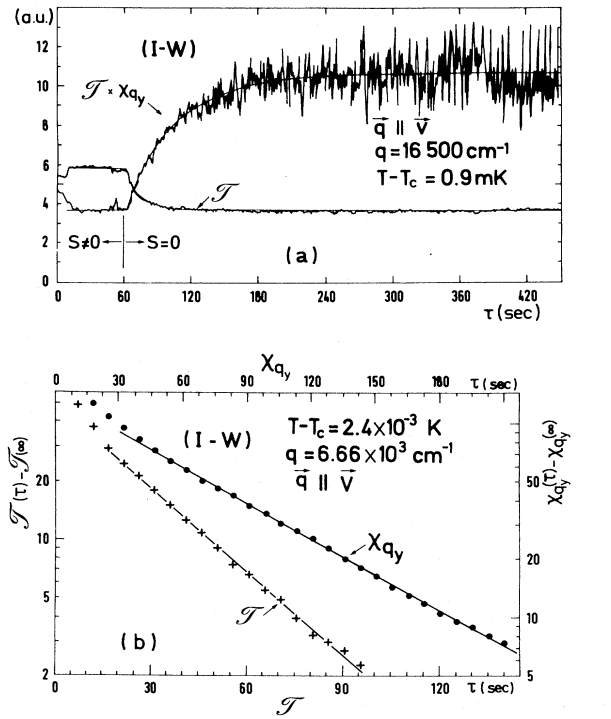

FIG. 13. (a) Transmission ($\mathcal{T}$) and rough scattered intensity ($\mathcal{T}\,\chi_{q_y}$) vs time, showing how the system perturbed by the shear recovers the equilibrium. (b) Semilogarithm plot of $\mathcal{T}$ and χ_q vs time showing an exponential behavior with characteristic times 31 sec for $\mathcal{T}$ and 80 sec for χ_{q_y}.

$$S_n^2 C_\varphi^+ = (2.45\pm0.04)\times10^{-23}\ \text{cm}^3$$

$$\xi_0^+ = (2.65\pm0.07)\times10^{-8}\ \text{cm}\ .$$

The subscript φ means that the variable volume fraction φ has been used as an order parameter in the estimation of $(\partial n^2/\partial M)_{p,T}$.

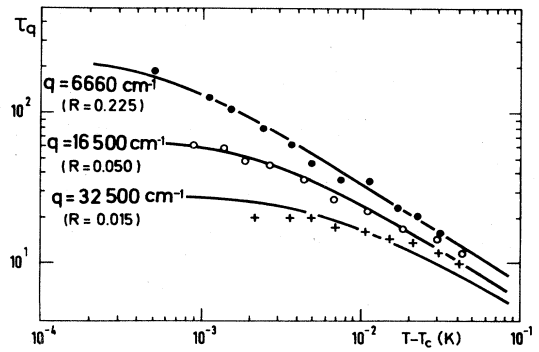

FIG. 14. Typical time τ_q vs $T - T_c$. The solid lines are the usual variations according to formula (47), where the amplitude R was adjustable.

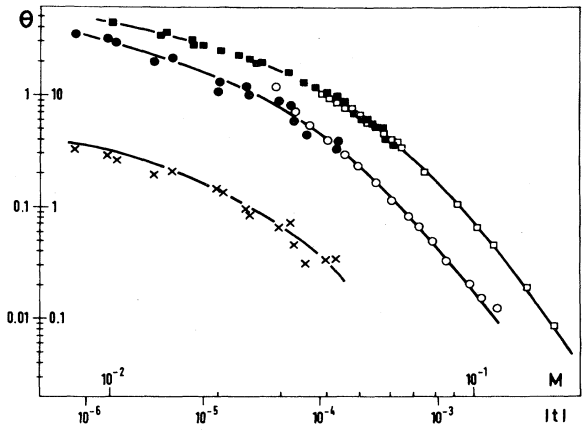

FIG. 15. Turbidity along the critical isochore above T_c (■ this work, □ from Ref. 14), along the coexistence curve (● this work, ○ from Ref. 11), and along the critical isotherm (× this work). The M and t scales are related by $M=B\,|\,t\,|^{\beta}$ with $B=0.77$. Inner scales are concerned with the critical isotherm.

2. *Coexistence curve below T_c*

The asymptotic values of the transmission correspond to the transmission on the coexistence curve, very close to the criticality. An analysis according to (30), changing t in $(M/B_0)^{1/\beta}$, gives

$$S_n^2 C_\varphi^- = (0.57\pm0.02)\times10^{-23}\ \text{cm}^3\ ,$$

$$\xi_0^- = (1.4\pm0.1)\times10^{-8}\ \text{cm}\ .$$

3. *Critical isotherm*

If we apply the coexistence curve equation (6), we determine the quantity $T_c - T_\varphi = T_c(M/B_0)^{1/\beta}$ and the transmission at T_c can be measured on the recordings. Again replacing t by $(M/B_0)^{1/\beta}$ in (30), the analysis of the data allows ξ_0' and $S_n^2 C_\varphi'$ to be measured:

$$S_n^2 C_\varphi' \equiv S_n^2(\delta D B^{\delta-1})^{-1} = (0.29\pm0.05)\times10^{-23}\ \text{cm}^3$$

$$\xi_0' \equiv \xi_0^c (B D^{1/\delta})^{-\nu/\beta} = (0.93\pm0.10)\times10^{-8}\ \text{cm}\ .$$

4. *Universal amplitude combinations*

Combining the results from IV G 1 to IV G 3 makes possible the estimation of the following ratios, whose theoretical value is in brackets (from the renormalization group or high temperature series approaches, respectively):

$$C^+/C^- = 4.3\pm0.3\ \ [4.5(\text{Ref. 15}),\ 5.03(\text{Ref. 16})]\ ,$$

$$\xi_0^+/\xi_0^- = 1.9\pm0.2\ \ [1.91(\text{Ref. 15}),\ 1.96(\text{Ref. 16})]\ ,$$

$$R_\chi^+ \equiv C^+ D B^{\delta-1} = 1.75\pm0.30\ \ [1.7(\text{Ref. 15})]\ ,$$

$$Q_2 \equiv \frac{C^+}{C_c}\left[\frac{\xi_0^c}{\xi_0^+}\right]^{2-\eta} = 1.1\pm0.3\ \ [1.21(\text{Ref. 13})]\ .$$

The agreement is fairly good with the theoretical combinations. For more details, see Refs. 7 and 14.

V. CONCLUSION

This work, initially devoted to the study of nonequilibrium critical fluids, has also allowed some interesting equilibrium properties to be obtained. We will summarize the main results obtained in these different fields.

A. Equilibrium properties

Both the susceptibility and the correlation length have been obtained above and below T_c at criticality and on the critical isotherm. These measurements have made possible the estimation of the universal combinations C^+/C^-, ξ_0^+/ξ_0^-, R_χ^+, and Q_2. The values are in good agreement with the theoretical expectations.

The time taken by the system to recover equilibrium after having been perturbed by a shear is seen to roughly behave with temperature as the diffusion time. However, there subsists an unexplained factor of 4 to 50 discrepancy with the amplitude calculated by the standard critical dynamics at equilibrium.

B. Out of equilibrium properties

The main object of this work was to clarify some misunderstood situations [see Ref. 3(c)]. After having studied under shear three different systems, at criticality or versus M, we can conclude that

(i) The shear affects the critical behavior of binary fluids in a region of M and T delimited by a crossover temperature $T_s(M)$, which varies as M^2, and a coexistence curve with the mean-field exponent $\beta^* = \frac{1}{2}$.

This region corresponds to the condition $S\tau > 1$, where the fluctuations have a lifetime τ large enough to "feel" the shear S. The amplitudes experimentally found are in fair agreement with the OK calculation.

(ii) There is a small but detectable change in the critical temperature, which is indirectly seen to vary with shear as $S^{1/3\nu} \simeq S^{0.53}$. The amplitude of this change is however 4 times smaller than expected from OK. This discrepancy could be attributed to the kind of shear which was experimentally produced, not strictly constant in direction.

(iii) The susceptibility at given wave vector q, shear S, order parameter M, and reduced tempera-

ture $t^* = (T - T_c^*)/T_c$ is well represented by the OK approximation:

$$\chi_q^{-1} \simeq a^* S^{\sigma_1}(t^*)^{\gamma^*} + b^* S^{\sigma_2} q_X^{\pi} + e^* S^{\sigma_3} M^{\gamma^*/\beta^*} + q^2 .$$

The exponents $\sigma_1 = (2\nu - 1)/3\nu \simeq 0.14$, $\sigma_3 = \frac{1}{3}$ have been determined indirectly and are in agreement with the above values. The exponents $\sigma_2 = \frac{8}{15}$ and $\pi = 0.4$ have been directly checked and experiments agree well with theory. The exponents γ^* and β^* exhibit the mean-field values 1 and $\frac{1}{2}$. Moreover the amplitudes a^*, b^*, and e^* are in reasonable agreement with the OK theory.

Finally the mean-field behavior was always seen to be relevant when the strong shear regime was reached.

It would be interesting to extend this study to other kinds of flow, such as the elongational flow where the effect should be more pronounced and where the absence of a mean velocity would allow the dynamics to be studied. Also the study of the phase separation process under shear could provide some new and unexpected phenomena. Experiments are in progress concerning this point.

ACKNOWLEDGMENTS

We are particularly indebted to C. Poitou and C. Poineau for help with the measurements, and G. Zalczer for fruitful discussions.

---

*Permanent address: Boîte Postale 404, Cotonou, Benin.

†Permanent address: E.S.H. Chott-Manem, Sousse, Tunisia.

[1]See, for instance, *Phase Transitions, Cargèse, 1980,* edited by M. Levy, J.-C. Le Guillou, and J. Zinn-Justin (Plenum Press, New York, 1982).

[2](a) A. Onuki and K. Kawasaki, Prog. Theor. Phys. Suppl. 64, 436 (1978); (b) A. Onuki and K. Kawasaki, Ann. Phys. N.Y. 121, 456 (1979); (c) A. Onuki, K. Yamazaki, and K. Kawasaki, Ann. Phys. N.Y. 131, 217 (1981).

[3](a) D. Beysens, M. Gbadamassi, and L. Boyer, Phys. Rev. Lett. 43, 1253 (1979); (b) D. Beysens and M. Gbadamassi, Phys. Rev. A 22, 2250 (1980); (c) D. Beysens, in Ref. 6.

[4]K. Kawasaki, Ann. Phys. (N.Y.) 61, 1 (1970).

[5]V. L. Ginzburg, Fiz. Tver. Tela (Leningrad) 2, 2031 (1960) [Sov. Phys. Solid State 2, 1824 (1960)].

[6]See, for instance, *Scattering Technique Applied to Supramolecular and Nonequilibrium Systems,* edited by S. H. Chen, B. Chu, and R. Nossal (Plenum Press, New York, 1981).

[7]D. Beysens, A. Bourgou, and P. Calmettes, Phys. Rev. A 26, 3589 (1982); see also Ref. 1.

[8]See, for instance, D. Beysens, J. Chem. Phys. 64, 2579 (1976) and Refs. therein.

[9]G. d'Arrigo, L. Mistura, and P. Tartaglia, J. Chem. Phys. 66, 80 (1977).

[10]D. Beysens, S. H. Chen, J. P. Chabrat, L. Letamendia, J. Rouch, and C. Vancamps, J. Phys. (Paris) Lett. 38, L203 (1977).

[11]D. Woermann and W. Sarholz, Ber. Bunsenges. Phys. Chem. 69, 319 (1965).

[12]M. Gbadamassi, Ph.D. thesis Université de Paris VI, 1982 (unpublished); Centre d'Etudes Nucléaires de Saclay Report No. DPh-T/SRM/82/33 (unpublished).

[13]J. P. Harnett, J. C. Y. Koh, and S. T. McComas, J. Heat Transfer 84, 82 (1962).

[14]G. Zalczer, A. Bourgou, and D. Beysens, Centre d'Etudes Nucléaires de Saclay Report No. DPh-T/SRM/82/34 (unpublished).

[15]E. Brézin, J.-C. Le Guillou, and J. Zinn-Justin, Phys. Lett. 47A, 285 (1974).

[16]H. B. Tarko and M. E. Fisher, Phys. Rev. B 11, 1217 (1975).